References

[1] Coenraad S, Toll MS, Hoeve HL, Goedegebure A. Auditory brainstem response morphology and analysis in very pre-term neonatal intensive care unit infants. Laryngoscope. 2011;121:2245–49.

[2] Crumpacker CS, Zhang JL. Cytomegalovirus. In: Mandell GL, Bennett JE, Dolin R, editors. Principles and practice of infectious diseases. 7th ed. Philadelphia: Elsevier; 2010. p. 1971–87.

[3] Dylewski J, Chou S, Merigan TC. Absence of detectable IgM antibody during cytomegalovirus disease in patients with AIDS. N Engl J Med. 1983;309:493.

[4] Gondo H, Minematsu T, Harada M, Akashi K, Hayashi S, Taniguchi S, et al. Cytomegalovirus (CMV) antigenaemia for rapid diagnosis and monitoring of CMV-associated disease after bone marrow transplantation. Br J Haematol. 1994;86:130–7.

[5] Griffiths PD, Stagno S, Pass RF, Smith RJ, Alford CA, Jr. Congenital cytomegalovirus infection: diagnostic and prognostic significance of the detection of specific immunoglobulin M antibodies in cord serum. Pediatrics. 1982;69:544–9.

[6] Inoue N, Koyano S. Evaluation of screening tests for congenital cytomegalovirus infection. Pediatr Infect Dis J. 2008;27:182–4.

[7] Kangro HO, Griffiths PD, Huber TJ, Heath RB. Specific IgM class antibody production following infection with cytomegalovirus. J Med Virol. 1982;10:203–12.

[8] Kawai T, Itoh Y, Hirabayashi Y, Ichihara K, Igarashi S, Iwata S, et al. Establishment of reference intervals and physiological parameters for 13 serum proteins in healthy Japanese adults. Jpn J Clin Pathol. 1996;44:429–34 (in Japanese).

[9] Kimberlin DW, Lin CY, Sanchez PJ, Demmler GJ, Dankner W, Shelton M, et al. Effect of ganciclovir therapy on hearing in symptomatic congenital cytomegalovirus disease involving the central nervous system: a randomized, controlled trial. J Pediatr. 2003;143:16–25.

[10] Koyano S, Inoue N, Oka A, Moriuchi H, Asano K, Ito Y, et al. Screening for congenital cytomegalovirus infection using newborn urine samples collected on filter paper: feasibility and outcomes from a multicentre study. Br Med J Open. 2011;1:e000118.

[11] Lanari M, Lazzarotto T, Venturi V, Papa I, Gabrielli L, Guerra B, et al. Neonatal cytomegalovirus blood load and risk of sequelae in symptomatic and asymptomatic congenitally infected newborns. Pediatrics. 2006;117:e76–83.

[12] Lazzarotto T, Lanari M. Why is cytomegalovirus the most frequent cause of congenital infection? Expert Rev Anti-Infe. 2011;9:841–3.

[13] Masuho Y, Matsumoto Y, Sugano T, Fujinaga S, Minamishima Y. Human monoclonal antibodies neutralizing human cytomegalovirus. J Gen Virol. 1987;68:1457–61.

[14] Matsuo K, Morioka I, Oda M, Kobayashi Y, Nakamachi Y, Kawano S, et al. Quantitative evaluation of ventricular dilatation using computed tomography in infants with congenital cytomegalovirus infection. Brain Dev. 2014;36:10–5.

[15] Metz CE, Herman BA, Roe CA. Statistical comparison of two ROC-curve estimates obtained from partially-paired datasets. Med Decis Making. 1998;18:110–21.

[16] Minematsu T, Hosoda K, Minamishima Y. Evaluation of direct immunoperoxidase technique using F(ab')2 fractions of anti-cytomegalovirus human monoclonal antibody for enumeration of cytomegalovirus antigen-positive leukocytes. J Jpn Assoc Infect Dis. 1994;68:1278–84 (in Japanese).

[17] Nelson CT, Demmler GJ. Cytomegalovirus infection in the pregnant mother, fetus, and newborn infant. Clin Perinatol. 1997;24:151–60.

[18] Nelson CT, Istas AS, Wilkerson MK, Demmler GJ. PCR detection of cytomegalovirus DNA in serum as a diagnostic test for congenital cytomegalovirus infection. J Clin Microbiol. 1995;33:3317–8.

[19] Noyola DE, Demmler GJ, Nelson CT, Griesser C, Williamson WD, Atkins JT, et al. Early predictors of neurodevelopmental outcome in symptomatic congenital cytomegalovirus infection. J Pediatr. 2001;138:325–31.

[20] Pass RF, Fowler KB, Boppana SB, Britt WJ, Stagno S. Congenital cytomegalovirus infection following first trimester maternal infection: symptoms at birth and outcome. J Clin Virol. 2006;35:216–20.

[21] Rasmussen L, Kelsall D, Nelson R, Carney W, Hirsch M, Winston D, et al. Virus-specific IgG and IgM antibodies in normal and immunocompromised subjects infected with cytomegalovirus. J Infect Dis. 1982;145:191–9.

[22] Revello MG, Zavattoni M, Baldanti F, Sarasini A, Paolucci S, Gerna G. Diagnostic and prognostic value of human cytomegalovirus load and IgM antibody in blood of congenitally infected newborns. J Clin Virol. 1999;14:57–66.

[23] Schlesinger Y, Halle D, Eidelman AI, Reich D, Dayan D, Rudensky B, et al. Urine polymerase chain reaction as a screening tool for the detection of congenital cytomegalovirus infection. Arch Dis Child Fetal Neonatal Ed. 2003;88:F371–4.

[24] Sonoyama A, Ebina Y, Morioka I, Tanimura K, Morizane M, Tairaku S, et al. Low IgG avidity and ultrasound fetal abnormality predict congenital cytomegalovirus infection. J Med Virol. 2012;84:1928–33.

[25] Tanaka Y, Kanda Y, Kami M, Mori S, Hamaki T, Kusumi E, et al. Monitoring cytomegalovirus infection by antigenemia assay and two distinct plasma real-time PCR methods after hematopoietic stem cell transplantation. Bone Marrow Transpl. 2002;30:315–9.

[26] Tanaka N, Kimura H, Iida K, Saito Y, Tsuge I, Yoshimi A, et al. Quantitative analysis of cytomegalovirus load using a real-time PCR assay. J Med Virol. 2000;60:455–62.

[27] Watzinger F, Suda M, Preuner S, Baumgartinger R, Ebner K, Baskova L, et al. Real-time quantitative PCR assays for detection and monitoring of pathogenic human viruses in immunosuppressed pediatric patients. J Clin Microbiol. 2004;42:5189–98.

[28] Wong V, Chen WX, Wong KY. Short- and long-term outcome of severe neonatal nonhemolytic hyperbilirubinemia. J Child Neurol. 2006;21:309–15.

[29] Yagi M, Yamamori M, Morioka I, Yokoyama N, Honda S, Nakamura T, et al. VEGF 936C>T is predictive of threshold retinopathy of prematurity in Japanese infants with gestational age of 30 weeks or less. Res Reports Neonatol. 2011;1:5–11.

[30] Yolken RH, Leister FJ. Enzyme immunoassays for measurement of cytomegalovirus immunoglobulin M antibody. J Clin Microbiol. 1981;14:427–32.

Measurement of maternal cerebral tissue hemoglobin on near-infrared time-resolved spectroscopy in the peripartum period

Kazunao Suzuki[1], Hiroaki Itoh[1], Mari Mukai[1], Kaori Yamazaki[1], Toshiyuki Uchida[1], Hideki Maeda[2], Motoki Oda[2], Etsuko Yamaki[2], Hiroaki Suzuki[2] and Naohiro Kanayama[1]

[1]Department of Obstetrics and Gynecology, Hamamatsu University School of Medicine, and [2]Hamamatsu Photonics, Hamamatsu, Japan

Abstract

Aim: To measure cerebral tissue hemoglobin in uncomplicated and complicated pregnant women during the peripartum period.

Methods: Time-resolved spectroscopy (TRS-20) can measure absolute concentration of oxygenated, deoxygenated, and total tissue hemoglobin based on the transit time of individual photons. Therefore, we used TRS-20 to measured tissue hemoglobin in the hemi-prefrontal lobes of normotensive pregnant women with ($n = 51$) or without ($n = 19$) epidural anesthesia, hypertensive pregnant women with pre-eclampsia ($n = 10$), a pregnant woman with acute onset of hypertension soon after delivery, and a hypertensive woman after hemorrhagic stroke in delivery.

Results: Cyclic labor concomitant with intra-abdominal pressure caused synergistic elevation in cerebral tissue hemoglobin. In contrast, epidural anesthesia reduced the amplitude of the cyclic increase of cerebral tissue hemoglobin in normotensive pregnant women. Hypertension in labor due to pre-eclampsia increased the amplitude of synergistic elevation of cerebral tissue hemoglobin caused by cyclic labor and intra-abdominal pressure. A prolonged high basal level of cerebral tissue hemoglobin was observed in a case of acute onset of hypertension soon after delivery. A decrease in cerebral tissue hemoglobin in the hemi-prefrontal lobe was observed in a woman 2 h after the onset of hemorrhagic stroke in labor.

Conclusions: TRS-20 can detect specific changes in maternal cerebral tissue hemoglobin level in response to physiological and pathophysiological changes in delivery. Thus, it represents a promising new conventional tool for maternal cerebral monitoring in the peripartum period.

Key words: delivery, eclampsia, hypertension, near-infrared spectroscopy, pregnancy.

Introduction

Neurological disorders, such as eclampsia and stroke, are rare maternal complications, but they can reduce mobility and/or increase mortality in both mothers and newborns.[1-5] A previous autopsy study reported that the number of maternal deaths associated with brain lesions in pregnancy was high.[6,7] Mothers in labor are at high risk of neurological disorders, such as eclampsia and stroke. Moreover, neurological disorders sometimes manifested without a preceding hypertensive phase and solely with acute severe

1

headache and/or visual disturbances.[8] Therefore, it is important to develop a system for maternal brain monitoring to protect against neurological disorders in deliveries. Nevertheless, a conventional and clear methodology has not yet been established for the early detection of neurological disorders in parturition apart from the measurement of blood pressure.[9]

Tissue oxygenation has been monitored using non-invasive measurement techniques, particularly near-infrared spectroscopy (NIRS),[10] to assess tissue damage in various clinical fields worldwide.[11,12] We measured the tissue oxygen index using NIRS and successfully assessed relative oxygenation of the human and porcine placenta in normal and pathological states, such as fetal growth restriction,[13,14] placental chorangiosis,[15] acute fetal hypoxia,[16] and pregnancy-induced hypertension.[17]

Radical changes have recently occurred in the monitoring of brain tissue oxygenation because of the use of NIRS to assess tissue oxygenation during anesthesia.[10,18-20] The different absorptive properties of oxygenated and deoxygenated hemoglobin (Hb) are used in NIRS to evaluate the metabolism of oxygen.[11,12] The absolute concentrations of oxygenated and deoxygenated Hb in target tissue, however, cannot be accurately determined or the relative status of tissue oxygenation assessed because the path-length cannot be measured.

In contrast, a new near-infrared time-resolved spectroscopy (TRS) system, TRS-20, has high data acquisition and can measure the absolute concentrations of oxygenated, deoxygenated, and total Hb by measuring the transit time of photons through the tissue of interest.[21-26] We recently successfully measured tissue oxygen saturation using TRS-20 by assessing the concentration of oxygenated, deoxygenated, and total Hb in the prefrontal lobes of the brains of pregnant women undergoing cesarean section before labor, and found that massive bleeding immediately and significantly decreased cerebral oxygen saturation.[27] It remains unknown, however, whether maternal cerebral oxygenated, deoxygenated, and total Hb levels change before, during, and after vaginal delivery.

In the present study, we measured tissue cerebral oxygenated, deoxygenated, and total Hb in the prefrontal lobes of normotensive pregnant women with or without epidural anesthesia, hypertensive pregnant women, a pregnant woman with acute onset of hypertension soon after vaginal delivery, and a hypertensive woman after hemorrhagic stroke in labor, and successfully showed that TRS-20 detected specific changes in maternal tissue Hb level in response to physiological and pathophysiological maternal conditions during the peripartum period.

Methods

Subjects

The subjects enrolled were normotensive pregnant women with (34.7 ± 4.5 years old, 39.2 ± 0.5 weeks of gestation, $n = 19$) or without (32.2 ± 4.8 years old, 39.6 ± 1.6 weeks of gestation, $n = 51$) epidural anesthesia and hypertensive pregnant women with pre-eclampsia (33.8 ± 5.1 years old, 38.4 ± 1.3 weeks of gestation, $n = 11$). They delivered vaginally at Hamamatsu University Hospital between June 2012 and April 2013. Informed consent was obtained after full explanation of the study. Pre-eclampsia was diagnosed prior to the onset of labor according to the American College of Obstetricians and Gynecologists (ACOG) Practice Bulletin (ACOG practice bulletin).[28] A 21-year-old pregnant woman was enrolled who delivered at 36 weeks 3 days of gestation and who had acute onset of hypertension soon after delivery. A 32-year-old woman was also enrolled who was transferred to Hamamatsu University Hospital from a local clinic 2 h after the estimated onset of hemorrhagic stroke in labor. Magnesium sulfate or antihypertensive medicine was not given during the measurement of cerebral oxygen saturation, except in a case of sudden onset of hypertension soon after delivery and in another case of maternal hemorrhagic stroke. Hypertensive pregnant women were excluded if magnesium sulfate and/or antihypertensive medicine was used before delivery. Subject background is summarized in Tables 1,2.

Measurements

Regional cerebral blood flow was estimated as previously described.[27] In brief, oxygenated Hb, deoxygenated Hb, and total Hb in the right prefrontal lobes were measured using TRS-20 (Hamamatsu Photonics, Hamamatsu, Japan).[21,22,27] Two fiber optic bundles (optodes), emitting and collecting near-infrared pulsed laser light, were fixed on the right side of the forehead of pregnant women with an interoptode distance of 4 cm. TRS-20 was used to evaluate oxygenation of the prefrontal lobes (Fig. 1) because hair could affect the transit time of each photon. The light source was a graded index type single fiber with a numerical aperture (NA) of 0.25 and a core that was 200 μm in diameter, and the light detector was a bundle of fibers with

Table 1 Subject background

	Age (years)	Weeks of gestation	SBP (mmHg)	DBP (mmHg)	Birthweight (g)
Normotensive pregnant women without epidural anesthesia ($n = 51$)	32.2 ± 4.8	39.6 ± 1.6	123.5 ± 10.7	76.4 ± 8.3	3139 ± 503
Hypertensive pregnant women with pre-eclampsia without epidural anesthesia ($n = 11$)	33.8 ± 5.1	38.4 ± 1.3#	157.8 ± 13.1*	94.1 ± 8.2*	2772 ± 621
Normotensive pregnant women with epidural anesthesia ($n = 19$)	34.7 ± 4.5	39.2 ± 0.5	119.9 ± 14.4	70.9 ± 7.3	3068 ± 409

#$P < 0.05$ vs normotensive pregnant women without epidural anesthesia; *$P < 0.01$ vs normotensive pregnant women with and without epidural anesthesia. DPB, diastolic blood pressure; SPB, systolic blood pressure.

Table 2 Complete hemogram

	RBC ($\times 10^4/\mu L$)	WBC ($/\mu L$)	Hemoglobin (g/dL)	Hematocrit (%)	PLT ($\times 10^4/\mu L$)
Normotensive pregnant women without epidural anesthesia ($n = 51$)	379 ± 34	9217 ± 2865	10.8 ± 1.2	33.4 ± 3.2	23.7 ± 5.1
Hypertensive pregnant women with pre-eclampsia without epidural anesthesia ($n = 11$)	426 ± 46*,†	7320 ± 2357	11.7 ± 0.9*,†	36.3 ± 2.8†	21.1 ± 5.9
Normotensive pregnant women with epidural anesthesia ($n = 19$)	365 ± 41	7498 ± 1459	10.7 ± 1.1	32.9 ± 3.1	22.4 ± 3.9

*$P < 0.05$ vs normotensive pregnant women without epidural anesthesia. †$P < 0.05$ vs normotensive pregnant women with epidural anesthesia. ††$P < 0.01$ vs normotensive pregnant women with epidural anesthesia. PLT, platelets; RBC, red blood cells; WBC, white blood cells.
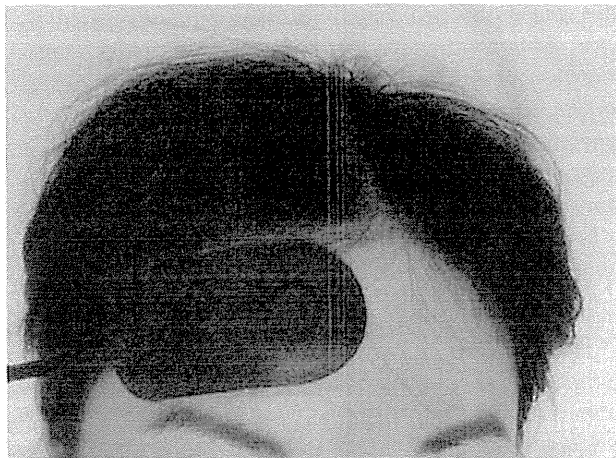

Figure 1 The near-infrared time-resolved spectroscopy (TRS) system, (TRS-20) optodes fixed on the right side of the forehead.

a diameter of 3 mm and NA of 0.26. A set of histograms of photon flight times, known as the re-emission profile, was recorded. One temporal re-emission profile included 1024 time channels spanning approximately 10 ns in steps of approximately 10 ps. In the present study, the emerging light was collected over a period of 10 s in order to exceed at least 1000 photons in the peak channel of the re-emission profiles. The instrumental response was measured with an input fiber placed opposite the receiving fiber through a neutral density filter. The instrumental response of the TRS-20 system was approximately 150 ps FWHM at each wavelength. The observed re-emission profiles were fitted to the photon diffusion equation[29] using the non-linear least square fitting method in order to determine the absorption coefficient (μ_a) and reduced scattering coefficient (μ_s') at each wavelength. Oxygenated Hb, deoxygenated Hb, total Hb, and the sum of oxygenated Hb and deoxygenated Hb were then calculated from the μ_a obtained at three wavelengths with the least square method.[30] The measurement started during the first stage of labor until approximately half an hour after delivery of the neonate.

Approval

This study was carried out with the approval of the Ethics Committee of Hamamatsu University School of Medicine (Number 24–33), which conforms to the provisions of the Declaration of Helsinki (as revised in Tokyo 2004).

3

Statistical analysis

Data are expressed as mean ± SD. The statistical significance of differences among three means was assessed using analysis of variance (ANOVA) followed by Scheffe's F-test or the Steel–Dwass test, as appropriate. $P < 0.05$ was regarded as significant.

Results

Effect of cyclic labor on cerebral tissue Hb during parturition

Intra-abdominal pressure is created by contraction of the abdominal muscles simultaneously with forced respiratory efforts with the glottis closed, and is necessary to complete the second stage of labor.[31] Intra-abdominal pressure is commonly observed during cyclic labor after full dilatation of the uterine cervix.[31]

Figure 2a shows representative changes in oxygenated Hb, deoxygenated Hb, and total Hb in the cerebral tissues of normotensive pregnant women. Cyclic labor did not affect cerebral tissue Hb before the occurrence of intra-abdominal pressure (Fig. 2a). In contrast, cyclic labor with intra-abdominal pressure synergistically elevated cerebral tissue Hb (Fig. 2a). Cyclic labor did not affect cerebral tissue oxygen saturation (data not shown).

Synergistic elevation in cerebral tissue Hb

During the second stage of labor after onset of intra-abdominal pressure, the amplitude of synergistic elevation in cerebral tissue total Hb by cyclic labor with intra-abdominal pressure was assessed using the formula {100 × (peak total tissue Hb – basal total tissue Hb)/(basal total tissue Hb)} and the value was expressed as a percentage. In normotensive pregnant women under epidural anesthesia, the mean amplitude of synergistic elevation in cerebral tissue total Hb by cyclic labor with intra-abdominal pressure (4.6 ± 1.6%, $n = 19$) was significantly lower than that in normotensive pregnant women without epidural anesthesia (8.5 ± 2.7%, $n = 51$, $P < 0.01$; Fig. 3).

Cerebral tissue Hb

Similar synergistic amplification in cerebral tissue Hb by cyclic labor with intra-abdominal pressure was observed in hypertensive pregnant women (Fig. 2c),
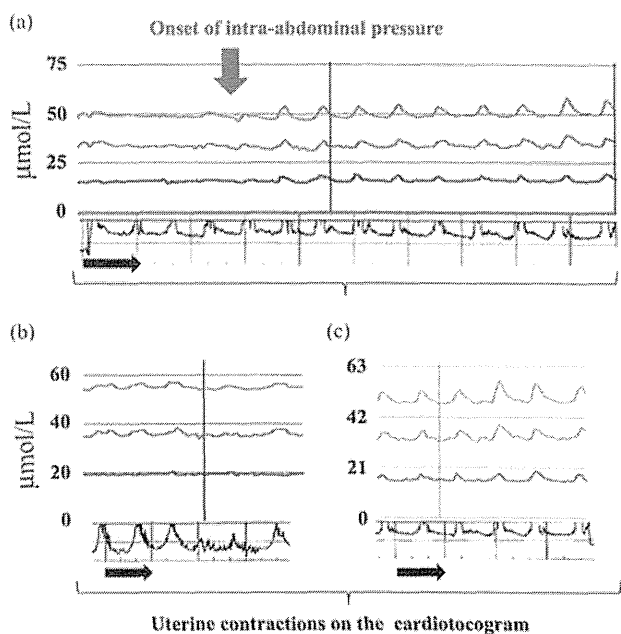

Figure 2 Representative changes in cerebral (red) oxygenated, (blue) deoxygenated, and (green) total tissue hemoglobin level in cyclic labor. (a) A normotensive pregnant woman at around the onset of intra-abdominal pressure; (b) a normotensive pregnant woman under epidural anesthesia soon before delivery; and (c) a hypertensive pregnant woman after the onset of intra-abdominal pressure. Black arrows, 3 min; red arrow, onset of intra-abdominal pressure.
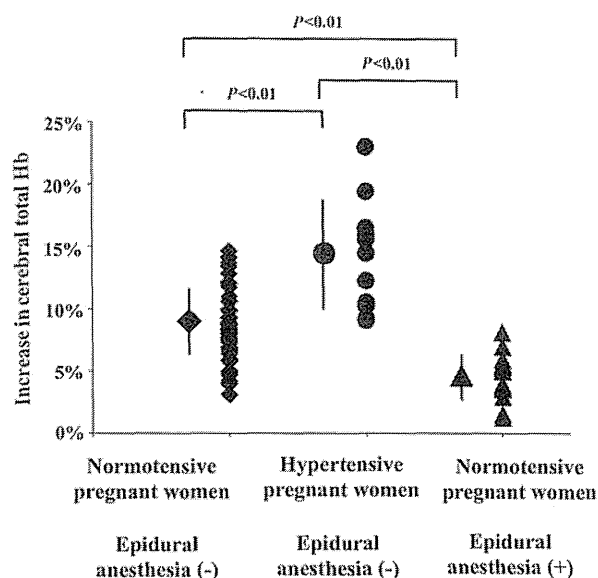

Figure 3 Amplitude of synergistic increase of cerebral total hemoglobin (Hb) by cyclic labor and intra-abdominal pressure. The amplitude of the increase was assessed using the formula {100 × (peak total tissue hemoglobin – basal total tissue hemoglobin)/(basal total tissue hemoglobin)}, and the value expressed as a percentage.

but the mean amplitude of synergistic elevation in cerebral tissue total Hb ($14.2 \pm 4.4\%$, $n = 11$) was significantly higher than that in normotensive pregnant women ($8.5 \pm 2.7\%$, $n = 51$, $P < 0.01$; Fig. 3).

Slightly prolonged high basal cerebral tissue Hb was observed in a case of acute onset of hypertension soon after delivery (Fig. 5).

Cerebral tissue Hb started to be monitored after the patient was transferred to our hospital, 2 h after the expected onset of hemorrhagic stroke in the left brain following hypertension in labor. On admission, cerebral tissue Hb in the left prefrontal lobe was lower than on the right (Fig. 4a). Vasogenic edema was observed in the occipital lobes on diffusion-weighted magnetic resonance imaging (MRI) 1 day after admission, and corresponded to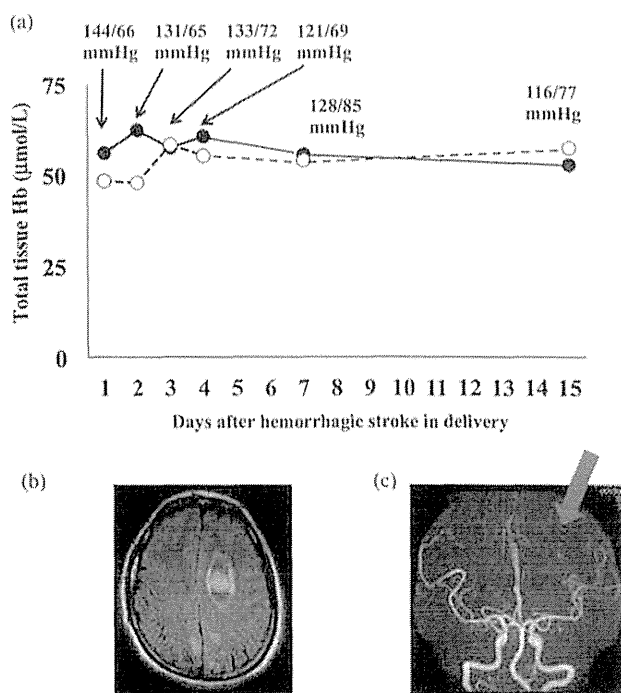 posterior reversible encephalopathy syndrome (Fig. 4b),[33] in which magnetic resonance angiography showed a decrease in blood flow to the left brain (Fig. 4c). Cerebral total Hb in the left prefrontal lobe recovered to that on the right side 7 days later (Fig. 4a).

Discussion

In the present study, we successfully measured tissue Hb in the prefrontal lobes of pregnant women in delivery using TRS-20. Cyclic labor did not affect cerebral tissue Hb in the relatively early stage of delivery (Fig. 2a). In contrast, in the second stage of delivery, typically after full dilatation of the uterine cervix, cyclic labor concomitant with intra-abdominal pressure synergistically elevated cerebral Hb (Fig. 2a), during which intra-abdominal pressure was created by contraction of the abdominal muscles simultaneously with forced respiratory efforts with the glottis closed.[31] Cyclic labor was shown to synergistically elevate oxygenated, deoxygenated, and total cerebral tissue Hb (Fig. 2), and, as a result, cerebral tissue oxygenation was stable in labor (data not shown).

The exact physiological meaning of this phenomenon has yet to be fully understood because we did not simultaneously assess maternal brain circulation on imaging, such as MRI. Therefore, an intensive assessment of maternal brain circulation in labor is necessary. Cyclic intra-abdominal pressure in the second stage of labor is very close to the cyclic Valsalva maneuver.[34–36] The Valsalva maneuver caused similar transient elevation in cerebral Hb in non-pregnant women and men (Suzuki K, Itoh H, Kanayama N, unpubl. obs., 2014). We speculated that a cyclic elevation in cerebral tissue Hb may be associated with changes in the autonomic nerve system because the Valsalva maneuver commonly causes transient sympathetic stimulation and parasympathetic nervous withdrawal.[36] Epidural anesthesia significantly reduced the amplitude of synergistic elevation in cerebral tissue Hb in normotensive pregnant women (Figs 2b,3). Because epidural anesthesia causes a reduction in sympathetic tone,[37] this result also supported the possibility that sympathetic stimulation by intra-abdominal pressure may be causatively connected with the synergistic elevation in cerebral tissue Hb.

The present study showed that the complication of pre-eclampsia significantly elevated the amplitude of the increase in synergistic elevation in cerebral tissue Hb caused by cyclic labor and intra-abdominal pressure (Figs 2c,3). Given that the Valsalva maneuver

Figure 4 (a) Basal cerebral total hemoglobin in a hypertensive pregnant woman with hemorrhagic stroke in labor. Measurements were started approximately 2 h after the expected onset of subarachnoid hemorrhage. Basal total hemoglobin in the (–●–) right and (- -○- -) left prefrontal lobes. (b) Diffusion-weighted magnetic resonance imaging 1 day after admission showing subarachnoid hemorrhage in the left cerebrum and vasogenic edema in the occipital region, which corresponded to posterior reversible encephalopathy syndrome.[32] (c) Red arrow, area of decreased blood flow around the hemorrhagic lesion in the left brain on magnetic resonance angiography 1 day after admission.

5

typically causes transient elevation in blood pressure,[36] we speculated that the increase in synergistic elevation of cerebral tissue Hb in pre-eclampsia may be associated with the transient elevation of maternal blood pressure during cyclic labor with intra-abdominal pressure. A prolonged high basal level of cerebral tissue Hb was observed in a case of acute onset of hypertension soon after delivery (Fig. 5). We did not measure maternal blood pressure continuously during cyclic labor; therefore, the possible involvement of an elevated maternal blood pressure in these phenomena will be examined in future studies.

The TRS-20 detected a decrease in cerebral tissue Hb in the hemi-prefrontal lobe in a woman 2 h after the onset of hemorrhagic stroke in labor (Fig. 4). Previous studies reported that TRS-20 could represent a promising sensor for assessing vasospasm associated with subarachnoid hemorrhage[38] as well as the effects of treatment for cerebral arteriovenous fistula.[39] It may be a promising candidate for conventional monitoring in order to provide timely information for clinical interventions against the onset of stroke, even in cases of unexpected sudden maternal deterioration among low-risk pregnant women; we did not, however, obtain this information during the onset of stroke. A large-scale cohort study is needed to clarify the sensitivity and specificity of TRS-20 for the onset of neurological disorders in parturition.
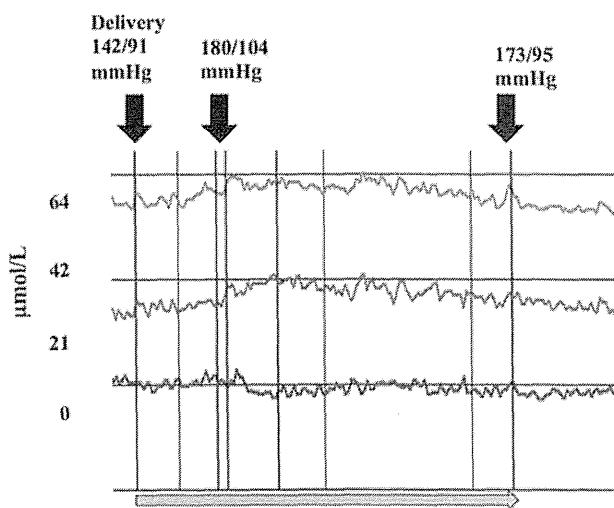
A limitation in the present study was the location of the two fiber optic bundles (optodes). They were fixed on the forehead of pregnant women (Fig. 1) to evaluate oxygenation saturation in the prefrontal lobes because hair could affect the transit time of each photon and this location was considered convenient for routine monitoring in delivery. Hypertension-associated brain edema, however, typically predominates in the parietal and occipital regions of the brain in pregnant women in labor.[40,41] Therefore, the aim of a future study is to compare cerebral oxygen saturation between the prefrontal and occipital lobes of hypertensive pregnant women. Another limitation is that we did not examine any cases of early or preceding detection of maternal neurological disorder using TRS-20. Therefore, a large-scale study is needed to evaluate the specificity and sensitivity of TRS-20 to detect neurological disorders in the peripartum period.

Conclusion

The TRS-20 could detect specific changes in maternal cerebral tissue Hb in response to physiological and pathophysiological conditions during the peripartum period and represents a promising new conventional tool for monitoring maternal brain circulation in labor, not only for high-risk, but also for low-risk pregnant women.

Acknowledgments

Disclosure

The authors declare no conflict of interest.

Figure 5 Changes in cerebral (red) oxygenated, (blue) deoxygenated, and (green) total tissue hemoglobin during the acute onset of maternal hypertension soon after delivery. Slightly prolonged high cerebral tissue hemoglobin was observed. Gray arrow, 30 min.

References

1. Berg CJ, Chang J, Callaghan WM, Whitehead SJ. Pregnancy-related mortality in the United States, 1991–1997. *Obstet Gynecol* 2003; **101**: 289–296.
2. Berg CJ, Harper MA, Atkinson SM *et al.* Preventability of pregnancy-related deaths: Results of a state-wide review. *Obstet Gynecol* 2005; **106**: 1228–1234.

3. Cunningham FG, Leveno KJ, Bloom SL, Hauth SL, Rousei DJ, Spng CY. Neurological and psychiatric disorders. In: *Williams Obstetrics*, 23rd edn. New York: McGraw-Hill, 2010; 1164–1184.
4. Khan M, Wasay M. Haemorrhagic strokes in pregnancy and puerperium. *Int J Stroke* 2013; 8: 265–272.
5. Bushnell C, Chireau M. Preeclampsia and stroke: Risks during and after pregnancy. *Stroke Res Treat* 2011; 2011: 858134.
6. Melrose EB. Maternal deaths at King Edward VIII Hospital, Durban. A review of 258 consecutive cases. *S Afr Med J* 1984; 65: 161–165.
7. Richards A, Graham D, Bullock R. Clinicopathological study of neurological complications due to hypertensive disorders of pregnancy. *J Neurol Neurosurg Psychiatry* 1988; 51: 416–421.
8. Veltkamp R, Kupsch A, Polasek J, Yousry TA, Pfister HW. Late onset postpartum eclampsia without pre-eclamptic prodromi: Clinical and neuroradiological presentation in two patients. *J Neurol Neurosurg Psychiatry* 2000; 69: 824–827.
9. Ghulmiyyah L, Sibai B. Maternal mortality from preeclampsia/eclampsia. *Semin Perinatol* 2012; 36: 56–59.
10. Jobsis FF. Noninvasive, infrared monitoring of cerebral and myocardial oxygen sufficiency and circulatory parameters. *Science* 1977; 198: 1264–1267.
11. Mathieu D, Mani R. A review of the clinical significance of tissue hypoxia measurements in lower extremity wound management. *Int J Low Extrem Wounds* 2007; 6: 273–283.
12. Vardi M, Nini A. Near-infrared spectroscopy for evaluation of peripheral vascular disease. A systematic review of literature. *Eur J Vasc Endovasc Surg* 2008; 35: 68–74.
13. Kawamura T, Kakogawa J, Takeuchi Y *et al.* Measurement of placental oxygenation by transabdominal near-infrared spectroscopy. *Am J Perinatol* 2007; 24: 161–166.
14. Kakogawa J, Sumimoto K, Kawamura T, Minoura S, Kanayama N. Noninvasive monitoring of placental oxygenation by near-infrared spectroscopy. *Am J Perinatol* 2010; 27: 463–468.
15. Suzuki K, Itoh H, Kimura S *et al.* Chorangiosis and placental oxygenation. *Congenit Anom (Kyoto)* 2009; 49: 71–76.
16. Suzukin K, Itoh H, Muramatsu K *et al.* Transient ligation of umbilical vessels elevates placental tissue oxygen index (TOI) values measured by near-infrared spectroscopy (NIRS) in clawn miniature pig animal model. *Clin Exp Obstet Gynecol* 2012; 39: 293–298.
17. Kakogawa J, Sumimoto K, Kawamura T, Minoura S, Kanayama N. Transabdominal measurement of placental oxygenation by near-infrared spectroscopy. *Am J Perinatol* 2010; 27: 25–29.
18. Lovell AT, Owen-Reece H, Elwell CE, Smith M, Goldstone JC. Predicting oscillation in arterial saturation from cardiorespiratory variables. Implications for the measurement of cerebral blood flow with NIRS during anaesthesia. *Adv Exp Med Biol* 1997; 428: 629–638.
19. Lovell AT, Owen-Reece H, Elwell CE, Smith M, Goldstone JC. Continuous measurement of cerebral oxygenation by NIRS during induction of anaesthesia. *Adv Exp Med Biol* 1997; 428: 213–218.
20. Madsen PL, Secher NH. Near-infrared oximetry of the brain. *Prog Neurobiol* 1999; 58: 541–560.

21. Oda M, Yamashita Y, Nakano T *et al.* Near infrared time-resolved spectroscopy system for tissue oxygenation monitor oxygenation monitor. *SPIE* 1999; 3597: 611–617.
22. Oda M, Yamashita Y, Nakano T *et al.* Near infrared time-resolved spectroscopy system for tissue oxygenation monitor. *SPIE* 2000; 4160: 204–210.
23. Hamaoka T, Katsumura T, Murase N *et al.* Quantification of ischemic muscle deoxygenation by near infrared time-resolved spectroscopy. *J Biomed Opt* 2000; 5: 102–105.
24. Ijichi S, Kusaka T, Isobe K *et al.* Quantification of cerebral hemoglobin as a function of oxygenation using near-infrared time-resolved spectroscopy in a piglet model of hypoxia. *J Biomed Opt* 2005; 10: 024026.
25. Ijichi S, Kusaka T, Isobe K *et al.* Developmental changes of optical properties in neonates determined by near-infrared time-resolved spectroscopy. *Pediatr Res* 2005; 58: 568–573.
26. Yamada E, Kusaka T, Arima N, Isobe K, Yamamoto T, Itoh S. Relationship between muscle oxygenation and electromyography activity during sustained isometric contraction. *Clin Physiol Funct Imaging* 2008; 28: 216–221.
27. Yamazaki K, Suzuki K, Itoh H *et al.* Cerebral oxygen saturation evaluated by near-infrared time-resolved spectroscopy (TRS) in pregnant women during caesarean section – a promising new method of maternal monitoring. *Clin Physiol Funct Imaging* 2013; 33: 109–116.
28. ACOG practice bulletin. Diagnosis and management of pre-eclampsia and eclampsia. Number 33, January 2002. *Obstet Gynecol* 2002; 99: 159–167.
29. Patterson MS, Chance B, Wilson BC. Time resolved reflectance and transmittance for the non-invasive measurement of tissue optical properties. *Appl Opt* 1989; 28: 2331–2336.
30. Ohmae E, Oda M, Suzuki T *et al.* Clinical evaluation of time-resolved spectroscopy by measuring cerebral hemodynamics during cardiopulmonary bypass surgery. *J Biomed Opt* 2007; 12: 062112.
31. Cunningham FG, Leveno KJ, Bloom SL, Hauth SL, Rousei DJ, Spng CY. Parturition. In: *Williams Obstetrics*, 23rd edn. New York: McGraw-Hill, 2010; 136–172.
32. Kinoshita T, Moritani T, Shrier DA *et al.* Diffusion-weighted MR imaging of posterior reversible leukoencephalopathy syndrome: A pictorial essay. *Clin Imaging* 2003; 27: 307–315.
33. Stevens CJ, Heran MK. The many faces of posterior reversible encephalopathy syndrome. *Br J Radiol* 2012; 85: 1566–1575.
34. Nishimura RA, Tajik AJ. The Valsalva maneuver and response revisited. *Mayo Clin Proc* 1986; 61: 211–217.
35. van Kraaij DJ, Jansen RW, Bouwels LH, Go RI, Verheugt FW, Hoefnagels WH. Use of Valsalva's maneuver to detect early recurrence of congestive heart failure in a randomized trial of furosemide withdrawal in older patients. *J Am Geriatr Soc* 1999; 47: 1384–1385.
36. Soucek M, Frana P, Kara T *et al.* The effect of short-term isometric muscle contraction and the Valsalva maneuver on systemic and pulmonary hemodynamics in patients with severe heart failure. *Clin Cardiol* 2009; 32: E32–E39.
37. Silva M, Halpern SH. Epidural analgesia for labor: Current techniques. *Local Regional Anesth* 2010; 3: 143–153.
38. Yokose N, Sakatani K, Murata Y *et al.* Bedside assessment of cerebral vasospasms after subarachnoid hemorrhage by near

7

infrared time-resolved spectroscopy. *Adv Exp Med Biol* 2010; **662**: 505–511.

39. Hoshino T, Sakatani K, Yokose N *et al.* Changes in cerebral blood oxygenation and hemodynamics after endovascular treatment of vascular malformation measured by time-resolved spectroscopy. *Adv Exp Med Biol* 2010; **662**: 491–496.

40. Bartynski WS. Posterior reversible encephalopathy syndrome, part 1: Fundamental imaging and clinical features. *AJNR Am J Neuroradiol* 2008; **29**: 1036–1042.

41. Cunningham FG, Leveno KJ, Bloom SL, Hauth SL, Rousei DJ, Spng CY. Pregnancy hypertension. In: *Williams Obstetrics*, 23rd edn. New York: McGraw-Hill, 2010; 706–756.

Amlodipine Passage into Breast Milk in Lactating Women with Pregnancy-Induced Hypertension and Its Estimation of Infant Risk for Breastfeeding

Takafumi Naito, PhD[1]*, Naoko Kubono, BSc[1]*, Shuhei Deguchi, MSc[2], Masahisa Sugihara, BSc[2], Hiroaki Itoh, MD, PhD[3], Naohiro Kanayama, MD, PhD[3], and Junichi Kawakami, PhD[1]

Abstract

Background: Few clinical reports have been published on amlodipine passage into breast milk in lactating women.
Objectives: The aims of this study were to evaluate the plasma concentration of amlodipine and its passage into breast milk in lactating women with pregnancy-induced hypertension and to estimate the risk for breastfeeding infants.
Methods: Thirty-one lactating women receiving oral amlodipine once daily for pregnancy-induced hypertension were enrolled. Pre-dose plasma and milk concentrations of amlodipine were determined at day 6 or later after starting the medication. Relative infant dose (RID) as an infant risk for breastfeeding was calculated by dividing the infant dose via milk by the maternal dose.
Results: The mean maternal dose of amlodipine was 6.0 mg. The medians of the plasma and milk concentrations of amlodipine were 15.5 and 11.5 ng/mL, respectively. Interindividual variation was observed in the amlodipine dose and body weight–adjusted milk concentrations (interquartile range [IQR], 96.7-205 ng/mL per mg/kg). The median and IQR of the amlodipine concentration ratio of milk to plasma were 0.85 and 0.74 to 1.08, respectively. The medians of infant birth weight and daily amlodipine dose via milk were 2170 g and 4.2 µg/kg, respectively. The median of the RID of amlodipine was 4.2% (IQR, 3.1%-7.3%).
Conclusion: Lactating women with pregnancy-induced hypertension had higher plasma concentrations of amlodipine during the early postpartum period. Oral amlodipine transferred into breast milk at the same level as that of plasma. However, the RID of amlodipine in most patients was less than 10%.

Keywords

amlodipine, breastfeeding, breast milk, pharmacokinetics, pregnancy-induced hypertension, relative infant dose

Well Established

Several case reports have indicated that maternal use of amlodipine during breastfeeding did not cause any adverse effects in breastfed infants. According to the LactMed Database, an alternative to amlodipine is preferred until more data become available.

Newly Expressed

Oral amlodipine was transferred into breast milk at the same level as that of plasma in lactating women with pregnancy-induced hypertension. However, the relative infant dose of amlodipine in most patients was less than 10%.

Background

Amlodipine, a long-acting dihydropyridine-type calcium channel blocker, is commonly used in the management of

hypertension and coronary artery disease.[1,2] Dihydropyridine-type calcium channel blockers that include amlodipine are empirically used for pregnancy-induced hypertension (PIH) in postpartum women based on their stable and strong

[1]Department of Hospital Pharmacy, Hamamatsu University School of Medicine, Hamamatsu, Shizuoka, Japan
[2]Biological Research Department, Sawai Pharmaceutical Co, Ltd, Osaka, Osaka, Japan
[3]Department of Obstetrics and Gynecology, Hamamatsu University School of Medicine, Hamamatsu, Shizuoka, Japan
*These authors contributed equally to this work.

Date submitted: August 21, 2014; Date accepted: October 28, 2014.

Corresponding Author:
Takafumi Naito, Vice-director, PhD, Department of Hospital Pharmacy, Hamamatsu University School of Medicine, 1-20-1 Handayama, Higashi-ku, Hamamatsu, Shizuoka 431-3192, Japan.
Email: naitou@hama-med.ac.jp

depressive effect.[3,4] According to the US National Library of Medicine LactMed Database,[5] an alternative to amlodipine is preferred until more data become available. However, limited information indicates that maternal use of amlodipine during breastfeeding has not caused any adverse effects in breastfed infants.[6-8]

Few clinical reports have been published on the passage of amlodipine into breast milk in lactating women. Factors that favor drug passage into milk are a low serum protein binding, high lipid solubility, and lack of charge at physiological pH.[9] Following oral administration, amlodipine is extensively metabolized via hepatic cytochrome P450 (CYP) 3A4[10] and slowly disappears with an elimination half-life of 34 hours.[11] The serum protein binding of amlodipine is 98%, and its distribution volume is 21 L/kg. The serum albumin level decreases during pregnancy and reaches a nadir toward the end of the pregnancy.[12] In addition, pregnancy induces the hepatic activity of CYP3A4.[13,14] However, the pharmacokinetic characteristics of amlodipine in lactating women remain to be clarified.

There have been no well-designed studies assessing the effects of maternally administered antihypertensive drugs delivered via breast milk in infants. Relative infant dose (RID) gives a good estimate of the amount of maternal dose received by the infant.[15] The RID is calculated by dividing the theoretical infant body weight–adjusted dose supplied via breast milk by the maternal body weight–adjusted dose. When the RID is less than 10% of the maternal dose, the medication is considered generally safe for breastfeeding.[15] Studies on nifedipine suggested a low RID of 2.3% with normal growth and no adverse effects in infants.[16,17] In case reports, the plasma concentration of amlodipine in infants was not detectable after breastfeeding for 4 days.[6] Few clinical studies have reported on the RID of amlodipine in lactating women.

Generally, breastfeeding is beneficial to both the mother and her infant; additionally, the medication for PIH in postpartum women is needed from the viewpoint of prevention of maternal organ failure. The aim of this study was to evaluate the plasma concentration of amlodipine and its passage into breast milk in lactating women with PIH and to estimate the infant risk for breastfeeding.

Methods

Patients and Study Schedule

The present study was an observation study (UMIN-CTR UMIN000013632) conducted at a single site at Hamamatsu University Hospital. Thirty-seven Japanese patients receiving orally disintegrating tablets of amlodipine besilate (Sawai Pharmaceutical Co, Ltd, Osaka, Japan) for PIH after delivery were recruited. After recruitment, 6 patients who had difficulty in collecting breast milk were excluded. Thus, 31 lactating women were enrolled in the study. Each patient received 5 mg amlodipine once daily as an initial

dose. The amlodipine dose was changed according to blood pressure goals (less than 140/90 mmHg) after delivery. Exclusion criteria were as follows: patients (1) who were being co-treated with a macrolide antibiotic or rifampin, (2) on hemodialysis or peritoneal dialysis, (3) who had hepatopathy (total bilirubin > 2.0 mg/dL), and (4) with poor compliance with respect to their medications. Blood and milk samplings were performed at day 6 or later after starting the medication. Specimens were collected within 3 weeks after the delivery. Two mL blood specimens were drawn into tubes containing EDTA 2Na at 24 hours after the morning dosing. A milk specimen of approximately 20 mL was collected into maternal milk storage bags at the time when the blood was sampled. In addition, infant characteristics and circulatory problems in breastfed infants were examined during the study period. The study was performed in accordance with the Declaration of Helsinki and its amendments, and the protocol was approved by the Ethics Committee of Hamamatsu University School of Medicine. The patients received information about the scientific aim of the study, and each patient provided written informed consent.

Determination of Amlodipine in Human Specimens

Amlodipine besilate was purchased from Sanyo Chemical Laboratory Co, Ltd (Osaka, Japan). Amlodipine-d7 maleate as an internal standard was synthesized by Sawai Pharmaceutical Co, Ltd. All other reagents were analytical grade and commercially available. Plasma was separated by centrifugation of the EDTA blood samples. For sample preparations, amlodipine in plasma and milk specimens was cleaned up by liquid phase extraction using methyl tert-butyl ether containing an internal standard. Amlodipine in the plasma and milk was determined using a gradient LC-MS/MS system with an electrospray ionization interface to the LC (API5000 triple-quadrupole MS, AB Sciex, Framingham, MA, USA). The intra- and inter-assay accuracies of amlodipine were 101.5% to 107.8% and 100.4% to 102.8% in human plasma and 96.9% to 110.8% and 102.0% to 104.6% in human milk, respectively. The intra- and inter-assay precisions of amlodipine were 1.2% to 5.6% and 0.9% to 5.1% in human plasma and 2.6% to 5.2% and 3.4% to 6.1% in human milk, respectively. The lower limits of quantification for amlodipine in human plasma and milk were 100 and 50 pg/mL, respectively.

Plasma and Milk Concentrations

The plasma and milk concentrations of amlodipine were evaluated as the pre-dose concentration and its dose and body weight–adjusted values. The concentration ratio of milk to plasma (M/P ratio) of amlodipine was calculated using their pre-dose concentrations.

Table 1. Maternal Characteristics (N = 31).

	Median (Interquartile Range)
Maternal age, y	35 (31-37)
Body weight after delivery, kg	61.4 (53.9-66.4)
Vaginal delivery/Caesarean section	7/24
Primipara/multipara	20/11
Gestational age, wk.d	36 wk 2 d (34 wk 5 d-37 wk 3 d)
Systolic blood pressure before treatment, mmHg	152 (146-162)
Diastolic blood pressure before treatment, mmHg	94 (89-100)
Serum albumin, g/L	26 (23-28)
Serum creatinine, mg/dL	0.68 (0.59-0.79)
Aspartate aminotransferase, IU/L	23 (19-40)
Alanine aminotransferase, IU/L	15 (8-23)

Relative Infant Dose

The daily volume of milk intake in infants has been estimated as 150 mL/kg.[18] The daily dose of amlodipine ingested by an infant via milk was obtained by multiplying the amlodipine concentration in milk by the daily volume of milk intake by the infant. The RID as an infant risk for breastfeeding was calculated from the following equation: RID (%) = $(C_{milk} \times V_{milk} / D_{maternal}) \times 100\%$, where C_{milk} is amlodipine concentration in milk (mg/mL); V_{milk}, daily volume of intake milk in infant; and $D_{maternal}$, body weight–adjusted amlodipine daily dose in mother (mg/kg).[15]

Statistical Analysis

All statistical analyses were performed using SPSS (15.0J, SPSS Japan Inc, Tokyo). All values are expressed as the median and interquartile range (IQR) except for the maternal dose of amlodipine.

Results

Maternal Characteristics

Table 1 shows the patient characteristics in 31 Japanese lactating women with PIH. The medians of systolic and diastolic blood pressure before the amlodipine treatment were 152 mmHg and 94 mmHg, respectively. No patient in the sample had smoked during the 6 months prior to study enrollment. The median and IQR of the serum albumin level were 26 and 23 to 28 g/L, respectively. The mean maternal dose of amlodipine and its body weight–adjusted value were 6.01 ± 2.31 mg and 0.0987 ± 0.0366 mg/kg, respectively. Blood and milk specimens were collected at day 10 (IQR, day 8-10) after starting the medication.

Figure 1. Plasma Concentration of Amlodipine in 31 Lactating Women with Pregnancy-Induced Hypertension.
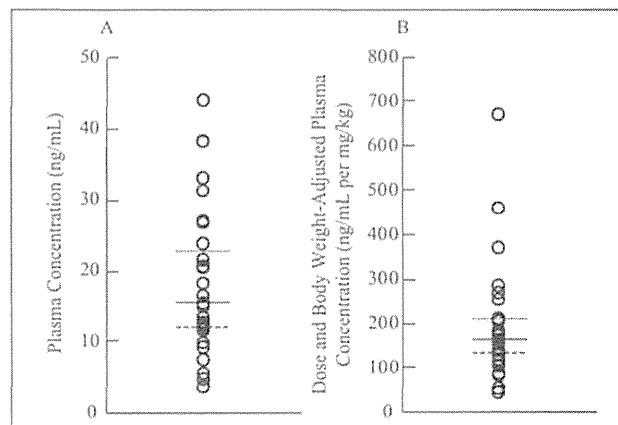
(A) Predose plasma concentration and (B) its dose and body weight–adjusted value. The bars represent the median (———) and 25th (– – – –) and 75th (·········) percentiles of the plasma concentration.

Figure 2. Milk Concentration of Amlodipine in 31 Lactating Women with Pregnancy-Induced Hypertension.
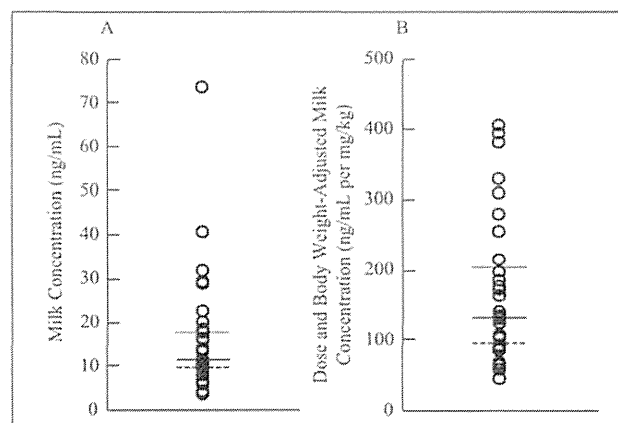
(A) Predose milk concentration and (B) its dose and body weight–adjusted value. The bars represent the median (———) and 25th (– – – –) and 75th (·········) percentiles of the milk concentration.
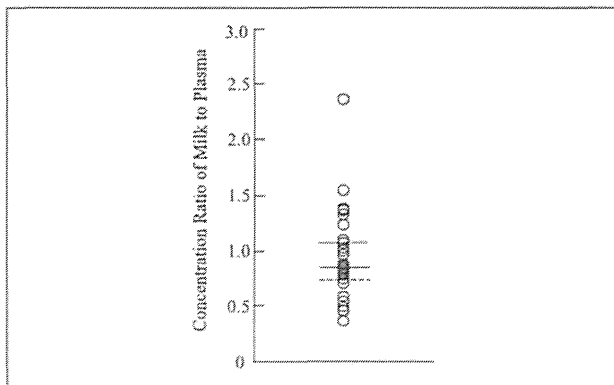
Plasma Concentration

Figure 1 shows the plasma concentration of amlodipine in 31 lactating women with PIH. The median of predose plasma concentrations of amlodipine was 15.5 ng/mL. Interindividual variability was observed in the predose plasma concentration of amlodipine in this study population (IQR, 12.0-22.8 ng/mL). The median and IQR of dose and body weight–adjusted predose plasma concentrations of amlodipine were 165 and 135 to 209 ng/mL per mg/kg, respectively.

Passage into Breast Milk

Figure 2 shows the milk concentration of amlodipine in 31 lactating women with PIH. The median of the predose milk

Figure 3. Amlodipine Concentration Ratio of Milk to Plasma Just before Dosing in 31 Lactating Women with Pregnancy-Induced Hypertension.

The bars represent the median (———) and 25th (– – – –) and 75th (·········) percentiles of the concentration ratio of milk to plasma.

Figure 4. The Relative Infant Dose of Amlodipine Just before Dosing in 31 Lactating Women with Pregnancy-Induced Hypertension.

The bars represent the median (———) and 25th (– – – –) and 75th (·········) percentiles of the relative infant dose.

concentration of amlodipine was 11.5 ng/mL. There was interindividual variability in the predose milk concentration in this study population (IQR, 9.84-18.0 ng/mL). The median and IQR of the dose and body weight–adjusted predose milk concentrations of amlodipine were 133 and 96.7 to 205 ng/mL per mg/kg, respectively. Figure 3 shows the M/P ratio of amlodipine at pre-dosing in 31 lactating women with PIH. The median and IQR of the M/P ratio of amlodipine were 0.850 and 0.743 to 1.08, respectively.
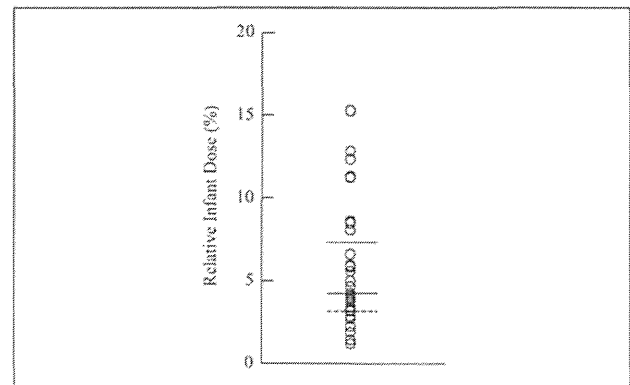
Estimation of Infant Risk for Breastfeeding

The median and IQR of infant birth weight were 2170 g and 1904 to 2635 g, respectively (n = 31). No problems in newborns were observed at birth except for transient respiration disorder. All infants had started breastfeeding by the time of the maternal blood and milk samplings. The daily dose of amlodipine in the infant via breast milk was 4.17 µg/kg (IQR, 3.05-6.32 µg/kg). Figure 4 shows the RID of amlodipine at pre-dosing in lactating women with PIH. The median and IQR of the amlodipine RID were 4.18% and 3.12% to 7.25%, respectively. In 26 of the 31 mothers, the RID of amlodipine was less than 10%. The maximum value of the amlodipine RID in this study population was 15.2%. No circulatory problems were observed in the breastfed infants during the maternal use of amlodipine in the study period.

Discussion

Several case reports have indicated that maternal use of amlodipine during breastfeeding did not cause any adverse effects in breastfed infants.[6-8] To date, no clinical studies have been published on the passage of amlodipine into breast milk in lactating women. This study investigated the plasma concentration of amlodipine and its passage into breast milk

in lactating women with PIH and estimated the infant risk for breastfeeding. Lactating women had higher plasma concentrations of amlodipine during the early postpartum period. The medians of the M/P ratio and RID of amlodipine were 0.85% and 4.2%, respectively. These findings suggest that oral amlodipine transfers into breast milk in lactating women. However, the RID of amlodipine in most patients was less than 10%. To the best of our knowledge, this is the first report that has evaluated the passage of amlodipine into breast milk and its RID.

The pharmacokinetic characteristics of amlodipine in lactating women are unclear. The plasma concentration of amlodipine was 15.5 ng/mL in these lactating women. The plasma concentration in lactating women was reported to be 2-fold higher than that in patients with essential hypertension.[19] In the present study, all enrolled lactating women had hypoalbuminemia (serum albumin level, 26 g/L). Pregnancy induces the activity of CYP3A4 in the liver.[13,14] Although pregnancy seemed to increase the clearance of amlodipine, the plasma concentration of amlodipine was heightened during the early postpartum period. The pharmacokinetic characteristics of amlodipine during the early postpartum period may be different from that during pregnancy. Our data suggest that lactating women possess higher plasma concentrations of amlodipine during the early postpartum period.

Few clinical studies have been published on the passage of amlodipine into breast milk in lactating women. The milk concentration and M/P ratio of amlodipine were 11.5 ng/mL and 0.85, respectively. Amlodipine transferred into breast milk at the same level as that into plasma in lactating women with PIH. The pKa of amlodipine is 8.7,[20] and drugs with a higher pKa generally have a higher M/P ratio because of the lower pH of milk, which is less than 7.2.[21] Amlodipine has higher lipid solubility than nifedipine.[11] Compared with nifedipine, which is an alternative drug according to the US

National Library of Medicine LactMed Database, amlodipine may more readily be transferred into milk based on factors that favor drug passage into milk.[9] In addition, interindividual variation was observed in the M/P ratio of amlodipine in this study population. In lactating women with hypoalbuminemia, the protein binding of amlodipine in plasma and milk pH may be responsible for the interindividual variation in the M/P ratio.

No well-designed clinical studies that assessed the infant effects of maternally administered amlodipine delivered via breast milk have been published. In this study, the RID of amlodipine was 4.2%. In 26 of the 31 lactating women, the RID of amlodipine was less than 10%, which is probably safe for use in breastfeeding mothers. The maximum RID of amlodipine was 15.2%. Even if the RID of breastfed drugs is greater than 10%, drugs with a low toxicity and no reported adverse effects in infants are acceptable for use in breastfeeding mothers.[22] In a case report, the plasma concentration of amlodipine in infants was not detectable after breastfeeding.[6] Case reports have indicated that maternal use of amlodipine during breastfeeding did not cause any adverse effects in breastfed infants.[6-8] In this study population, maternal use of amlodipine did not cause any circulatory problems during the study period (within 3 weeks after delivery) after delivery in breastfed infants.

The present study has several limitations. First, we investigated the RID of amlodipine during the early postpartum period in lactating women. Human breast milk changes in composition from colostrum to late lactation.[23] The RID of amlodipine during early postpartum may be different from that during late postpartum. However, in most patients, PIH gradually improved after delivery and the medication had been withdrawn. Second, it examined the pre-dose plasma and milk concentrations of amlodipine. The maximum milk concentration of amlodipine may be higher than the pre-dose milk concentration of amlodipine. Drug passage into breast milk occurs generally due to simple passive diffusion and pH gradients.[24] This passage property indicates that amlodipine concentration in milk is correlated with that in plasma of breastfeeding mothers. The M/P and RID values for amlodipine in this study could be considered reliable due to its long-acting and high distribution properties. Further studies that include multiple milk samplings would clarify the RID of amlodipine in breastfeeding mothers.

Infant safety during maternal amlodipine use while breastfeeding has not been fully clarified in clinical settings. Although it was difficult to investigate the adverse effects on long-term breastfeeding in infants, no circulatory problems were observed in breastfed infants during maternal use of amlodipine. Several case reports concluded that the maternal use of amlodipine during breastfeeding most likely did not have an effect on infant growth.[6-8] This study demonstrated the short-term safety of amlodipine in breastfeeding mothers during the early postpartum period. For long-term breastfeeding, assessment of the RID and plasma concentration of

amlodipine in infants may be needed from the viewpoint of infant safety. Further studies that also include infant growth would help confirm the safety of amlodipine in breastfeeding mothers.

Conclusion

Lactating women with PIH had a higher plasma concentration of amlodipine during the early postpartum period. Oral amlodipine was transferred into breast milk at the same level as that of plasma in this study population. However, the RID of amlodipine in most patients was less than 10%.

Declaration of Conflicting Interests

Funding

References

1. Murdoch D, Heel RC. Amlodipine. A review of its pharmacodynamic and pharmacokinetic properties, and therapeutic use in cardiovascular disease. *Drugs*. 1991;41(6):478-505.
2. Clavijo GA, de Clavijo IV, Weart CW. Amlodipine: a new calcium antagonist. *Am J Hosp Pharm*. 1994;51(1):59-68.
3. Ghanem FA, Movahed A. Use of antihypertensive drugs during pregnancy and lactation. *Cardiovasc Ther*. 2008;26(1): 38-49.
4. Ghuman N, Rheiner J, Tendler BE, White WB. Hypertension in the postpartum woman: clinical update for the hypertension specialist. *J Clin Hypertens*. 2009;11(12):726-733.
5. US National Library of Medicine, National Institutes of Health, Health & Human Services. Drugs and Lactation Database (LactMed) website. http://toxnet.nlm.nih.gov/cgi-bin/sis/htmlgen?LACT. Accessed August 22, 2014.
6. Vasa R, Martha Ramirez M. Amlodipine exposure through breastfeeding in a 32 week preterm newborn. *Breastfeeding Med*. 2013;8(suppl 1):S15.
7. Ahn HK, Nava-Ocampo AA, Han JY, et al. Exposure to amlodipine in the first trimester of pregnancy and during breastfeeding. *Hypertens Pregnancy*. 2007;26(2):179-187.
8. Szucs KA, Axline SE, Rosenman MB. Maternal membranous glomerulonephritis and successful exclusive breastfeeding. *Breastfeed Med*. 2010;5(3):123-126.
9. Podymow T, August P. Update on the use of antihypertensive drugs in pregnancy. *Hypertension*. 2008;51(4):960-969.
10. Zhu Y, Wang F, Li Q, et al. Amlodipine metabolism in human liver microsomes and roles of CYP3A4/5 in the dihydropyridine dehydrogenation. *Drug Metab Dispos*. 2014;42(2): 245-249.
11. Faulkner JK, McGibney D, Chasseaud LF, Perry JL, Taylor IW. The pharmacokinetics of amlodipine in healthy volunteers after single intravenous and oral doses and after 14 repeated

oral doses given once daily. *Br J Clin Pharmacol.* 1986;22(1):21-25.

12. Elliott JR, O'Kell RT. Normal clinical chemical values for pregnant women at term. *Clin Chem.* 1971;17(3):156-157.

13. Anderson GD. Using pharmacokinetics to predict the effects of pregnancy and maternal-infant transfer of drugs during lactation. *Expert Opin Drug Metab Toxicol.* 2006;2(6):947-960.

14. Papageorgiou I, Grepper S, Unadkat JD. Induction of hepatic CYP3A enzymes by pregnancy-related hormones: studies in human hepatocytes and hepatic cell lines. *Drug Metab Dispos.* 2013;41(2):281-290.

15. Nice FJ, Luo AC. Medications and breast-feeding: current concepts. *J Am Pharm Assoc.* 2012;52(1):86-94.

16. Ehrenkranz RA, Ackerman BA, Hulse JD. Nifedipine transfer into human milk. *J Pediatr.* 1989;114(3):478-480.

17. Penny WJ, Lewis MJ. Nifedipine is excreted in human milk. *Eur J Clin Pharmacol.* 1989;36(4):427-428.

18. Bennet PN. *Drugs and Human Lactation.* Amsterdam, Netherlands: Elsevier; 1988:325-326.

19. Fujiwara T, Ii Y, Hatsuzawa J, et al. The Phase III, double-blind, parallel-group controlled study of amlodipine 10 mg once daily in Japanese patients with essential hypertension who insufficiently responded to amlodipine 5 mg once daily. *J Hum Hypertens.* 2009;23(8):521-529.

20. van Zwieten PA. Amlodipine: an overview of its pharmacodynamic and pharmacokinetic properties. *Clin Cardiol.* 1994;17(9 suppl 3):III3-6.

21. Marks JM, Spatz DL. Medications and lactation: what PNPs need to know. *J Pediatr Health Care.* 2003;17(6):311-317.

22. Hale TW. *Medications and Mother's Milk 2012. 15th ed. A Manual of Lactational Pharmacology.* Plano, TX: Hale Publishing; 2012:7-19.

23. Ballard O, Morrow AL. Human milk composition: nutrients and bioactive factors. *Pediatr Clin North Am.* 2013;60(1):49-74.

24. Atkinson HC, Begg EJ. Prediction of drug distribution into human milk from physicochemical characteristics. *Clin Pharmacokinet.* 1990;18(2):151-167.

Examiner's finger-mounted fetal tissue oximetry

Naohiro Kanayama
Masatsugu Niwayama

Examiner's finger-mounted fetal tissue oximetry

Naohiro Kanayama[a,*] and Masatsugu Niwayama[b,c]
[a]Hamamatsu University School of Medicine, Department of Obstetrics and Gynecology, Hamamatsu 431-3192 Japan
[b]Shizuoka University, Department of Electrical and Electronics Engineering, Hamamatsu 431-3192 Japan
[c]Shizuoka University, Research Institute of Electronics, Hamamatsu 431-3192 Japan

Abstract. The best way to assess fetal condition is to observe the oxygen status of the fetus (as well as to assess the condition of infants, children, and adults). Previously, several fetal oximeters have been developed; however, no instrument has been utilized in clinical practice because of the low-capturing rate of the fetal oxygen saturation. To overcome the problem, we developed a doctor's finger-mounted fetal tissue oximeter, whose sensor volume is one hundredth of the conventional one. Additionally, we prepared transparent gloves. The calculation algorithm of the hemoglobin concentration was derived from the light propagation analysis based on the transport theory. We measured neonatal and fetal oxygen saturation (StO_2) with the new tissue oximeter. Neonatal StO_2 was measured at any position of the head regardless of amount of hair. Neonatal StO_2 was found to be around 77%. Fetal StO_2 was detected in every position of the fetal head during labor regardless of the presence of labor pain. Fetal StO_2 without labor pain was around 70% in the first stage of labor and around 60% in the second stage of labor. We concluded that our new concept of fetal tissue oximetry would be useful for detecting fetal StO_2 in any condition of the fetus. © *The Authors. Published by SPIE under a Creative Commons Attribution 3.0 Unported License. Distribution or reproduction of this work in whole or in part requires full attribution of the original publication, including its DOI.* [DOI: 10.1117/1.JBO.19.6.067008]

Keywords: fetal tissue oximetry; finger pulp; examiner; near-infrared spectroscopy; parturition.

Paper 130788RR received Nov. 5, 2013; revised manuscript received May 13, 2014; accepted for publication May 16, 2014; published online Jun. 24, 2014.

1 Introduction

Fetal heart rate (FHR) monitoring is a popular worldwide method to evaluate the condition of the fetus. The best approach to diagnose the fetal condition is to measure the fetal blood pressure and oxygen status, which at the moment, cannot be achieved noninvasively. The FHR is the gold standard in evaluating the fetal condition, however, the FHR monitoring has shown low false-negative and high-false positive rates. Thus, obstetricians have attempted to measure the fetal oxygen status instead of or in addition to the FHR monitoring. As a result, there have been many reports on the development and clinical trials of the fetal pulse oximetry.

The pulse oximetry enables us to determine the degree of oxygen saturation both noninvasively and continuously by measuring pulsating wave absorbance in the peripheral tissues, such as fingertips. Some researchers have reported that the oxygen dynamics can be measured over the course of delivery using a pulse oximetry probe applied transvaginally to the fetal head.[1–3] Moreover, the intravaginal optical probe for tissue oximetry using the near-infrared spectroscopy (NIRS) has been developed.[4,5] However, the sensor volume of 4 cm^3 (diameter 1 cm, length 5 cm) was too large to apply during delivery. The dimensions of the commercially available small optical probes for the brain (NIRO-200NX, Hamamatsu Photonics, Hamamatsu, Japan) and the muscle (Hb-14, ASTEM, Kawasaki, Japan) were $1 \times 3 \times 0.5$ cm (width, length, and thickness). The sensors' volume of 1.5 cm^3 was too large for monitoring the fetus directly. Additionally, the significantly low data capturing rate is one of

the biggest drawbacks to these procedures. East et al. have reported that during the active phase of labor, every method has a significant rate of signal loss and the loss of sensor contact occurred up to 64% of time with oximetry.[6] Another drawback of this transvaginal procedure is that the probe often moves away from the fetal head during delivery, which may lead to an intrauterine infection caused by rupture of the gestational sac. Furthermore, these methods are essentially invasive, as the probe is inserted into the uterine cervix only after the rupture of the gestational sac. In addition to these problems, many patients feel discomforted by the intravaginal sensor. Obstetricians also feel that there is interference with the cervical examination by the sensor. Although many clinical trials of the fetal pulse oximetry have been performed, its clinical usefulness has been controversial. Thus, there are no established methods for detecting the fetal hypoxia during parturition yet. At present, many obstetricians look forward to further improvement of oximetry and a better understanding of clinical management.

We changed the conventional placement of sensors to overcome those problems. We proposed an idea of moving the sensor attachment from the fetus to the examiner. Namely, we attached an NIRS probe to the doctor's finger, instead of the fetal head or cheek. The obstetricians and midwives need to perform a cervical examination to understand the progress of delivery. They need to touch the fetal head to detect any cervical dilatation and the fetal position during delivery. Therefore, we hypothesized that if an NIRS probe was placed on the examiner's finger pulp and the appropriate calculation algorithms on the near field of the light source were developed, we could obtain the fetal oxygen status noninvasively. With this concept, we succeeded in attaching an NIRS probe to the examiner's finger pulp. Here, we report our intruments and preliminary clinical data.

*Address all correspondence to: Naohiro Kanayama, E-mail kanayama@hama-med.ac.jp

231

2 Instrumentation

An NIRS probe consists of near-infrared light emitting diodes (LEDs) and photodiodes. The source-detector distance was 4.0 cm in accordance with the Nelcore's fetal pulse oximetry (Nellcor N-400 system), which has been used in many clinical trials. We considered that if the distance could be shortened to around 1 cm, it would be possible to place the sensor on the examiner's finger. Our previous study showed that the strong signals of the arteries in the fetal scalp and brain surface were obtained at the point of 10 mm of the source-detector separation.[7] Therefore, we thought that the miniaturized sensor would detect a fetal oxygenation signal by (1) deriving the calculation algorithm of the hemoglobin concentration satisfied in the near field of the light source, (2) blocking light propagation to the examiner's finger to prevent it from mixing with the unwanted finger oxygenation, and (3) manufacturing an ultrathin optical probe which fits to the finger pulp. Fortunately, we successfully developed a new small volume sensor with a polyimide-based flexible substrate. The wavelengths of the light sources were 770 and 810 nm, and sensitivity of the photodiodes (PD2501, Kyoto, Epitex) was high in the near-infrared band. The bare chips of the LEDs and photodiodes were mounted on the substrate with a wire bonding. The detectors were located 6 and 8 mm away from the LEDs in order to determine an absolute value of the hemoglobin concentration using the spatially resolved NIRS [Fig 1(a)], which was created based on a laboratory-made low noise instrument.

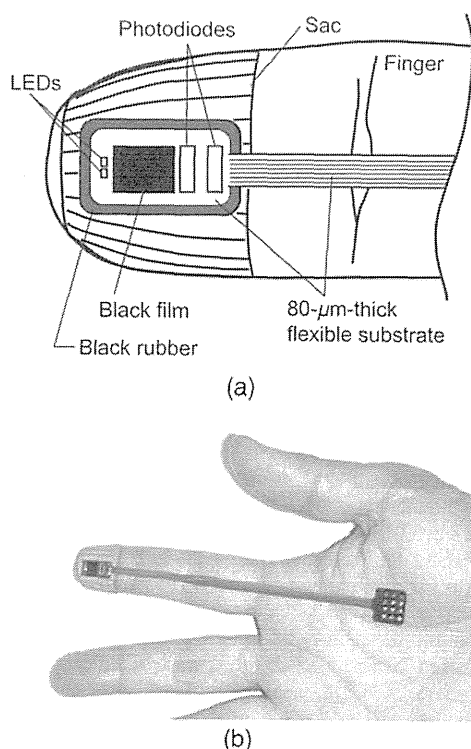We placed a 1-mm thick black rubber sheet between the optical probe and finger pulp to block the light scattered through the examiner's finger. Then, the probe was fixed with an adhesive sheet on the black-colored finger sac. The optical elements integrated with a flexible cable (80-μm thick, 100-mm long) were connected to a soft shield cable on the examiner's palm. A 1.5-m long shield line was connected to the microcomputer unit in the examiner's breast pocket. In order to reduce external noise, the unit was battery powered and had a 2.4 GHz wireless module. The measured data were wirelessly transmitted into the computer. The trend of the hemoglobin concentration processed[8] and calculated by the computer was shown on the screen in real time.

We prepared transparent vinyl gloves in collaboration with Utsunomiya Seisaku Co., Ltd. (Higashi Osaka-shi, Japan). The same amount of scattered light as without gloves was detected with the gloves. Figure 1(b) shows the examiner's finger with the developed optical probe.

3 Theoretical Analysis

We examined the light propagation in the fetal head model. The simulation model consists of the fetal scalp, skull, cerebrospinal fluid (CSF), brain, optical block, and examiner's finger. Table 1 shows the scattering coefficient, absorption coefficient, and thickness, which were set based on the literature data.[9-11]

The anisotropic factors for each layer were 0.95.[12] The propagation of photons in the simulation was based on the transport theory with the Monte Carlo method. The model was divided into small cubes, and the optical path lengths in each cube were calculated to examine the measurement sensitivity. Figure 2 presents the sensitivity distribution obtained from the simulation results.

The results suggest that the light propagated to the finger does not contribute to the detected light intensity. In the simulation, the absorption coefficient of the optical block attached to the finger was 10 mm^{-1}. The optical absorber of the actual probe was easily realized because a typical colored adhesive tape has an absorption coefficient from 1 to 20 mm^{-1}. The changes in spatial intensity slope were examined to reveal the measurement sensitivity for the brain and the scalp. The slope values of S_0, S_{brain}, and S_{scalp} represent an initial state ($\mu_{a\_\text{brain}} = 0.02$ mm^{-1}, $\mu_{a\_\text{scalp}} = 0.02$ mm^{-1}), a state where only the brain has changed ($\mu_{a\_\text{brain}} = 0.025$ mm^{-1}, $\mu_{a\_\text{scalp}} = 0.02$ mm^{-1}), and a state where only the scalp has changed ($\mu_{a\_\text{brain}} = 0.02$ mm^{-1}, $\mu_{a\_\text{scalp}} = 0.025$ mm^{-1}), respectively.

(a)

(b)

Fig. 1 Scheme (a) and photograph (b) of the oximeter probe attached to the examiner's finger pulp. Flexible substrate mounted two LEDs and two photodiodes are adhered to a black rubber sheet.

Table 1 Optical properties and thickness of each layer for Monte Carlo analysis.

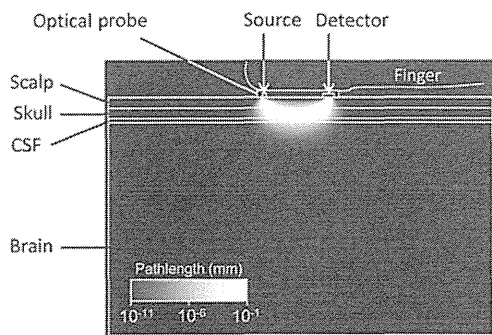| Tissue	Scattering coefficient μ_s (mm^{-1})	Absorption coefficient μ_a (mm^{-1})	Thickness (mm)
Scalp	26	0.00–0.050	1.5
Skull	40	0.010	1.5
Cerebrospinal fluid	8	0.002	0.4
Brain	32	0.00–0.050	100.0
Finger	26	0.020	10.0
Optical block	20	10.0	0.4

232

Fig. 2 Model for the Monte Carlo analysis and the sensitivity distribution obtained by the simulation.

The changes in slope were calculated as follows: $\Delta S_{brain} = S_{brain} - S_0$ and $\Delta S_{scalp} = S_{scalp} - S_0$. The sensitivity ratio was defined as $\Delta S_{brain}/\Delta S_{scalp}$. The ratio became high due to an increase in the source-detector distance, as shown in Fig. 3. When the detectors were located 6 and 8 mm from the light source, the sensitivities for the brain and the scalp were comparable. If the hemoglobin concentration of the brain is higher than that of the scalp, the values of the oxygen saturation and blood volume would contain more information about the brain than the scalp. Although the long source-detector distance was preferable in order to focus on measuring the cerebral tissue, we adopted the length of the 6 and 8 mm pair, considering convenience due to the size reduction.

In this study, the hemoglobin concentrations of both brain and scalp were measured. Therefore, we simultaneously varied the values of μ_{a_brain} and μ_{a_scalp} from 0.00 to 0.05 mm^{-1}. Then, we made a lookup table of the relationship between the value of μ_a and the spatial slope. In the measurement, the value of μ_a was calculated from the spatial slope of the measured light intensity using the lookup table. The following equations were used to calculate the concentrations of oxyhemoglobin [O$_2$Hb] and deoxyhemoglobin [HHb]:

$$[O_2Hb] = \frac{\varepsilon_{Hb}^{\lambda 2}\mu_a^{\lambda 1} - \varepsilon_{Hb}^{\lambda 1}\mu_a^{\lambda 2}}{\varepsilon_{HbO2}^{\lambda 1}\varepsilon_{Hb}^{\lambda 2} - \varepsilon_{HbO2}^{\lambda 2}\varepsilon_{Hb}^{\lambda 1}}, \tag{1}$$

$$[HHb] = -\frac{\varepsilon_{HbO2}^{\lambda 2}\mu_a^{\lambda 1} - \varepsilon_{HbO2}^{\lambda 1}\mu_a^{\lambda 2}}{\varepsilon_{HbO2}^{\lambda 1}\varepsilon_{Hb}^{\lambda 2} - \varepsilon_{HbO2}^{\lambda 2}\varepsilon_{Hb}^{\lambda 1}}, \tag{2}$$

where $\varepsilon_{HHb}^{\lambda 1,2}$ and $\varepsilon_{O2Hb}^{\lambda 1,2}$ are the extinction coefficients of HHb and O$_2$Hb, respectively, at the wavelengths $\lambda 1$ and $\lambda 2$.[13] Tissue oxygen saturation StO$_2$ was calculated by [O$_2$Hb]/([O$_2$Hb] + [HHb]).

4 Clinical Experiments

To determine whether our tissue oximetry obtained the fetal oxygenation, we measured StO$_2$ of three just delivered newborns at first. All the neonates were born in spontaneous vaginal delivery from 39 to 40 weeks of gestation. The FHR monitored during labor showed a reassuring fetal status pattern in all cases. The Apgar scores of the neonates were 9, 9, 10 at 1 min and 10, 10, 10 at 5 min. We attached the probe on the front hair, parietal, and occiput of head just after delivery. Each measurement lasted at least 10 s.

Second, we measured fetal StO$_2$ during labor, as shown in Fig. 4. We measured StO$_2$ for one parturient at the first and the second stages of labor after the rupture of membranes. The parturient was in her 39th week of pregnancy. The course of delivery was normal. The probe was attached to the fetus head during delivery. We examined the results for 2 min during the first and second stages of labor. We continued the measurement for 10 min after delivery. Informed consent was obtained from the subjects, and all measurements were approved by the ethical committee of Hamamatsu University School of Medicine.

The StO$_2$ values of the parietal region in the three newborns were 78.5 ± 2.6%, 78.4 ± 3.2%, and 75.8 ± 2.3%, respectively. The values of front and occiput were similar to those of the parietal region in each newborn (data not shown). We could obtain the StO$_2$ easily in any condition of the neonate head, such as wetness or color of the hair.

The intrapartum fetal StO$_2$ was detected through the whole delivery (Fig. 5).

The fetal StO$_2$ was detected even during labor pains and the bearing down effort. We obtained the StO$_2$ data smoothly and quickly. The doctor got the fetal StO$_2$ as well as the cervical findings at the same time. Furthermore, the patient felt neither pain nor discomfort during the measurement. The fetal StO$_2$ in
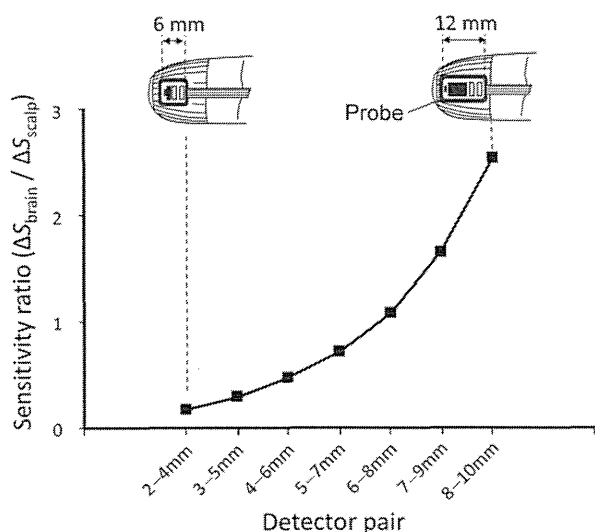

Fig. 3 Relationship between the brain-scalp sensitivity ratio and the pair of source-detector distances.
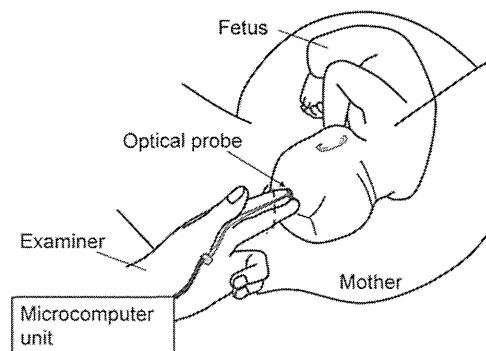

Fig. 4 Outlook of the measurement with an oximeter attached to the examiner's finger during labor.
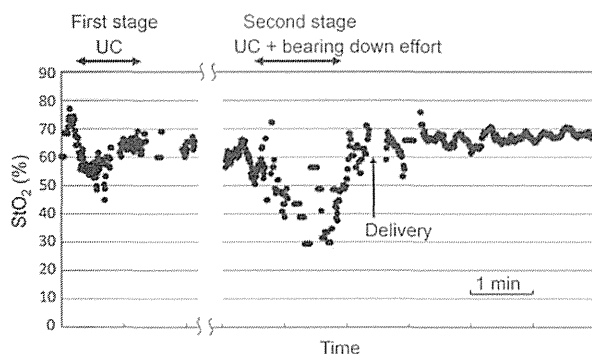
233

Fig. 5 The actual chart of the fetal StO_2 during labor. Left and right parts correspond to the first and the second stages of labor, respectively. UC denotes uterine contraction.

the first stage of labor was about 70% without labor pains and about 60% in a presence of labor pains. In the second stage of labor, the fetal SpO_2 was 60% without labor pains, and it decreased during labor pains and the bearing down effort. The lowest level of the fetal StO_2 was around 30%. After delivery, the neonate StO_2 increased rapidly up to 70%.

5 Discussion

All previous oximeter sensors were attached to the fetus. We have recognized the accidental possibility of the movement of the sensor and its slip during labor. Poor data capture was observed in some pregnant women due to the detachment of the sensor caused by frequent changes of the body position during labor.

Our oximetry system is able to detect the fetal StO_2 in the first and the second stages of labor very precisely regardless of the presence of labor pains. As the examiner can touch suitable sites during the internal examination, it is possible to measure the fetal StO_2 very naturally. Our fetal StO_2 measurements can be performed at the same time and in the same manner as obstetrical examinations during delivery. We recognized the fetal head promptly and obtained the fetal StO_2 precisely, because the pressure for an ultrathin probe propagated to the finger and the finger pulp was very sensitive. Furthermore, our sensor never touches the fetus directly because the sensor is inside the transparent sterilized gloves. We think that our measurement system is safer and more noninvasive than the previous one. Moreover, the parturient does not feel discomfort during the measurement.

As for the clinical analysis, the fetal StO_2 in the first stage of labor was about 70% without labor pains and about 60% in the presence of labor pains. The fetal oxygen saturation SpO_2 with a pulse oximeter is $59 \pm 10\%$ in the first stage of labor, and $53 \pm 10\%$ in the second stage.[2] The measurements of low saturation were estimated at 33% as two standard deviations below the mean. Since the decrease in arterial oxygenation rapidly results in low tissue oxygenation, the value of StO_2 would be correlated to SpO_2 strongly. Chipchase et al. have reported that the cerebral StO_2 for a fetus was $59 \pm 12\%$ using an optical fiber-based NIRS instrument.[14] The oxygen saturation values in this study were the same or slightly higher compared to the previous studies. One of the reasons would be that the value of StO_2 was a mixed measurement of the scalp and the brain. If the sensitivity of the scalp was suppressed by using a long separation probe, the values may be close to the cerebral oxygen saturation values

previously reported. The comparison of results suggests that our new concept of oximetry could be applicable to clinical practice.

In this study, there was no caput succedaneum in the fetal head. When the thickness of the caput succedaneum layer is thick, the cerebral sensitivity (the ratio of $\Delta S_{brain}/\Delta S_{scalp}$) would decrease. In the future, we may solve the problem of the swelling layer by squeezing the subcutaneous fluid and by measuring the surface layer thickness with an ultrasound apparatus.

As for neonatal monitoring, the values of cerebral StO_2 for a child and a neonate have been reported to range from 65% to 85%[15] and from 67% to 80%,[16,17] respectively. The oxygen saturation values in this study (75%–78%) were similar to that reported in the literature.

Fouzas et al. described that SpO_2 with a pulse oximeter might not be measured or might be inaccurate in low-perfusion states, such as low cardiac output, shock, hypothermia, vasoconstriction, and arterial occlusion.[18] They also stated that a continuous oxygen saturation monitoring is essentially needed for the safety of the newborn. Rapid measurements of several sites of StO_2 are needed in the case of neonatal asphyxia. But the commercially available sensor is set on one site of the skin of the neonate. Our sensor can be set on any site of the newborn where doctors want to measure. In addition, the spatially resolved NIRS system can detect the tissue oxygenation in a low-perfusion condition, because the StO_2 measurements require only the spatial intensity slope and do not require the weak pulsation signals on a pulse oximetry. Our system could be useful in practice for such cases. To assure the usefulness of this oximetry, we must accumulate more data. At the moment, we are planning a multicenter study to confirm the usefulness of our system.

In conclusion, we developed an oximeter with the sensors attached to the fingers of an obstetrician or a midwife, in contrast to conventional oximeters whose sensors were attached to the fetus. We successfully detected the fetal oxygenation smoothly and certainly. We are sure that our system could become a new fetal monitoring approach.

Acknowledgments

References

1. E. van Oudgaarden and N. Johnson, "Clinical value of antenatal fetal pulse oximetry," *J. Perinat. Med.* **22**(4), 295–300 (1994).
2. G. A. Dildy et al., "Intrapartum fetal pulse oximetry: fetal oxygen saturation trends during labor and relation to delivery outcome," *Am. J. Obstet. Gynecol.* **171**(3), 679–684 (1994).
3. G. A. Dildy, "Fetal pulse oximetry." *Clin. Obstet. Gynecol.* **54**(1), 66–73 (2011).
4. C. J. Aldrich et al., "Fetal cerebral oxygenation measured by near-infrared spectroscopy shortly before birth and acid-base status at birth," *Obstet. Gynecol.* **84**(5), 861–866 (1994).
5. S. Schmidt, "Laserspectroscopy in the fetus during labour." *Eur. J. Obstet. Gynecol. Reprod. Biol.* **110**(Suppl 1), S127–S131 (2003).
6. C. E. East et al., "Fetal pulse oximetry for fetal assessment in labour," *Cochrane. Database Syst. Rev.* **2**, CD004075 (2007).
7. N. Stuban, M. Niwayama, and H. Santha, "Phantom with pulsatile arteries to investigate the influence of blood vessel depth on pulse oximeter signal strength." *Sensors (Basel)* **12**(12), 895–904 (2012).

234